Journal of ELECTRONIC MATERIALS, Vol. 31, No. 10, 2002 *Special Issue Paper*

Transient-Enhanced Diffusion in Shallow-Junction Formation

A.T. FIORY,[1,6] S.G. CHAWDA,[1] S. MADISHETTY,[1] V.R. MEHTA,[1] N.M. RAVINDRA,[1] S.P. MCCOY,[2] M.E. LEFRANÇOIS,[2] K.K. BOURDELLE,[3] J.M. MCKINLEY,[3] H.-J.L. GOSSMANN,[4] and A. AGARWAL[5]

1.—Department of Physics, New Jersey Institute of Technology, Newark, NJ 07102. 2.—Vortek Industries, Vancouver, BC, Canada V6P 6T7. 3.—Agere Systems, Orlando, FL 32819. 4.—Agere Systems, Murray Hill, NJ 07974. 5.—Axcelis Technologies, Beverly, MA 01915. 6.—E-mail: anthony.fiory@njit.edu

Shallow junctions are formed in crystalline Si by low-energy ion implantation of B^+, P^+, or As^+ species accompanied by electrical activation of dopants by rapid thermal annealing and the special case of spike annealing. Diffusion depths were determined by secondary ion-mass spectroscopy (SIMS). Electrical activation was characterized by sheet resistance, Hall coefficient, and reverse-bias diode-leakage measurements. The B^+ and P^+ species exhibit transient-enhanced diffusion (TED) caused by transient excess populations of Si interstitials. The electrically activated fraction of implanted dopants depends mainly on the temperature for B^+ species, while for P^+ species, it depends on both temperature and P^+ dose. The relatively small amount of diffusion associated with As^+ implants is favorable for shallow-junction formation with spike annealing.

Key words: Ion implantation, spike annealing, electrical activation

INTRODUCTION

Current methods for forming junctions in the source and drain regions of complementary metal-oxide semiconductor (CMOS) transistor circuits use low-energy ion implantation and rapid thermal annealing (RTA). Spike annealing, with fast ramping and short dwell time at maximum temperature, has been shown to be advantageous for shallow-junction formation.[1] Diffusion and electrical activation of implanted B^+, P^+, and As^+ dopants in crystalline Si are examined in this work. During annealing, these dopants experience an enhanced diffusion when excess Si interstitials are present. For implanted-dopant species, excess Si interstitials evolve from the residual implant damage until the damage is annealed out. The resulting enhanced diffusion is, thus, transient and is denoted transient-enhanced diffusion (TED).[2–5] In the case of boron, excess interstitials can also be generated by the formation of a boron-silicide phase if the surface boron concentration is high enough.[6] The phenomenon is referred to as boron-enhanced diffusion (BED) and occurs for both ion-implanted B^+ and for a B film deposited on the surface.

Although enhanced diffusion of any kind is unfavorable for shallow-junction formation in advanced transistor designs, grain-boundary-enhanced diffusion is beneficial in gate-electrode formation from implanted polycrystalline Si.[7] The high temperatures reached by spike annealing are also advantageous for increasing the concentration of dopants in solid solution.[8]

(Received May 15, 2002; accepted July 8, 2002)

BORON IMPLANTS

Boron-concentration profiles were determined by secondary ion-mass spectroscopy (SIMS) for $^{11}B^+$ implants at four energies ranging from 0.5–5 keV and are shown in Fig. 1. Incandescent-lamp 1,050°C, 10-sec RTA was used to produce the annealing profiles. The annealed B-concentration distributions are characterized by a peak within 10 nm of the surface and a diffusive tail. Most of the boron in the peak near the surface is electrically inactive and believed to be in the form of clustered B or a silicon-boride phase, which can form if the peak concentra-

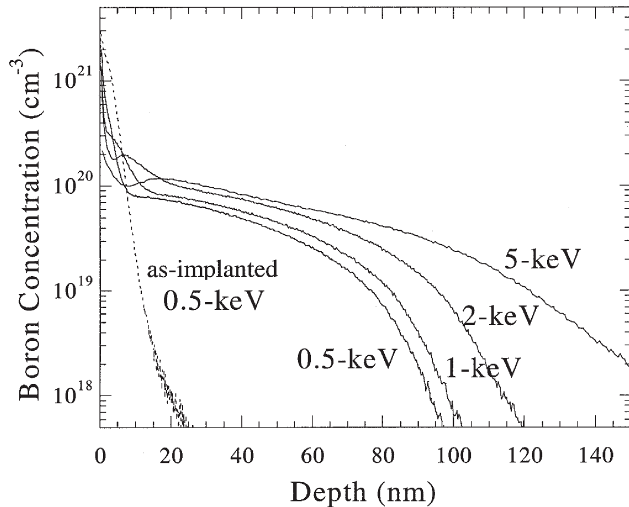

Fig. 1. The boron concentration versus depth from SIMS for $^{11}B^+$ implants of 10^{15} cm^{-3} dose at energies of 0.5 keV, 1 keV, 2 keV, and 5 keV and annealed at 1,050°C for 10 sec. The as-implanted profile for the 0.5-keV B^+ implant is also shown.

tion exceeds a few atomic percent, as is the case for 0.5-keV B^+. The B diffusivities estimated from the diffusion tails are greater than the equilibrium diffusivity of B at the anneal temperature.

Enhanced-B diffusion has been examined quantitatively from the thermal-diffusion broadening of B marker layers at 150-nm depth grown on Si samples by molecular-beam epitaxy.[6] The circle symbols in Fig. 2 give the diffusivity-enhancement factor as a function of implant range for various B implants after RTA at 1,050°C and 10 sec. The enhancement factor corresponding to the diamond symbol at zero range was obtained by annealing a B film deposited on a clean Si surface. The result for the deposited-film experiment verifies the trend that enhanced diffusion persists as implant energy and range approach zero. The remaining enhanced diffusion in the absence of implant damage is BED, caused by excess Si interstitials associated with high concentrations of B in Si.

Given that the diffusion of implanted-B dopants is not in thermal equilibrium, it is, nonetheless, instructive to consider a phenomenological mean diffusivity estimated from the diffusion depth and the anneal time. This was examined in an experiment in which the diffusion temperatures and times were mutually varied under the constraint that a constant portion of B is to be activated.[9] The experiment used a 0.75-keV, 10^{15} cm^{-2} B^+ implant in a wafer with a 2.1-nm thermal SiO_2 film. Samples were annealed by incandescent-lamp RTA in 0.1% O_2 ambient for times that were decreased as anneal temperatures were increased. Figure 3 shows the results for the mean diffusivity and the associated activation times on Arrhenius scales for a constant electrical activation of 53% of the B. The activation time is the effective time at the anneal temperature and includes corrections for the temperature transitions during heating (~150°C/sec) and cooling (~80°C/sec). The Arrhenius fit of the temperature-time relationship indicates an effective thermal-activation energy of 5.1 ± 0.1 eV. The thermal diffusivity of B, interpreted as an average over the anneal cycle, is fitted with an effective thermal-activation energy of 4.1 ± 0.1 eV. The approximately 1-eV lower thermal-activation energy for diffusion, relative to the time for activating a given fraction, indicates that spike anneals, with short time at high temperature, are favorable for suppressing diffusion of the B dopant.

Transient-diffusion effects cause the junction depth, X_J, to be dependent on ramp rate, when the ramp rate is sufficiently slow. This was studied for a 0.5-keV B implant by using spike anneals with a range of ramp-up rates from 50–400°C/sec. An electric arc-lamp heating method was used to produce sharply peaked spikes for each anneal.[10] Cooling

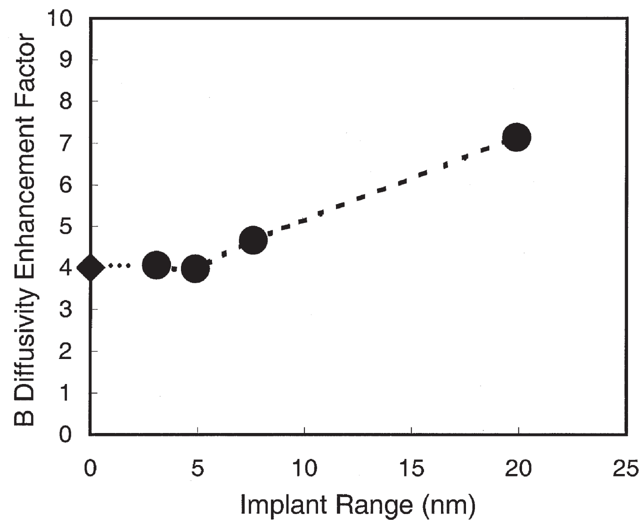

Fig. 2. The boron diffusivity-enhancement factors at 1,050°C. Circle symbols: 10^{15} cm^{-2} $^{11}B^+$ implants as a function of implant range for energies from 0.5–5 keV. Diamond symbol at zero range: B film-deposited and annealed.

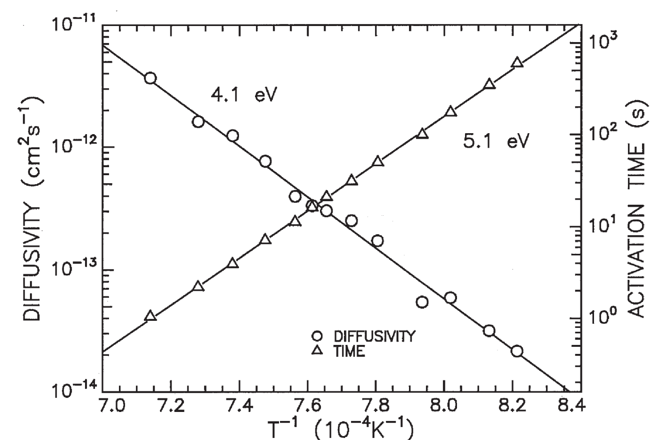

Fig. 3. The Arrhenius plots of mean B diffusivity (left scale) and activation time (right scale) for producing a fixed sheet-carrier density of 5.3×10^{14} cm^{-2} for a 0.75-keV B^+ implant at 10^{15} cm^{-2} dose. Dashed lines are fits with the thermal-activation energies of 4.1 eV for the diffusivity and 5.1 eV for the activation time.

rates, approximately 100°C/sec, were determined by free-wafer radiation absorbed by a black chamber. To compensate for the decrease in the effective thermal budget near the peak temperature with increasing ramp-up rate, the peak temperatures were adjusted to yield a constant value of sheet resistance, R_S = 550 Ω/Sq. The results for X_J, defined as the depth at which the B concentration equals 10^{18} cm^{-3} in SIMS profiles, are shown in Fig. 4. The data show that the junction depth and, thus, diffusion depth is nearly independent of ramp rate in the range of 100–400°C/sec. However, the junction depth is 12% deeper for the 50°C/sec ramp rate. One concludes from these observations that a ramp rate that is higher than 50°C/sec should be sufficient to suppress TED for this shallow B^+ implant.

The results of a study of the temperature and dose dependence for spike anneals of 0.5-keV B^+ implants are shown in Fig. 5. The electric arc-lamp method was used with a ramp rate of 400°C/sec. The general trend of the data is that the activated fraction of the B increases monotonically with temperature and remains relatively insensitive to the implant dose. Although BED was found to increase with implant dose in a previous study,[6] the variability in diffusivity appears to a have minor influence on the electrically active fraction.

Activation of implants can leave residual lattice defects near the range of the implanted ions. For anneals that generate sufficient dopant diffusion, the defects should be largely contained within the region of high carrier concentration and, thus, have minimal influence on junction properties. This was examined for the preceding anneals by diode-leakage currents measured at a reverse bias of −1 V. The substrate is n type with a doping level in the 10^{14} cm^{-3} range. The measurements used wet, chemically etched, diode mesas, approximately 1 mm in diameter. Up to four diodes were measured for each

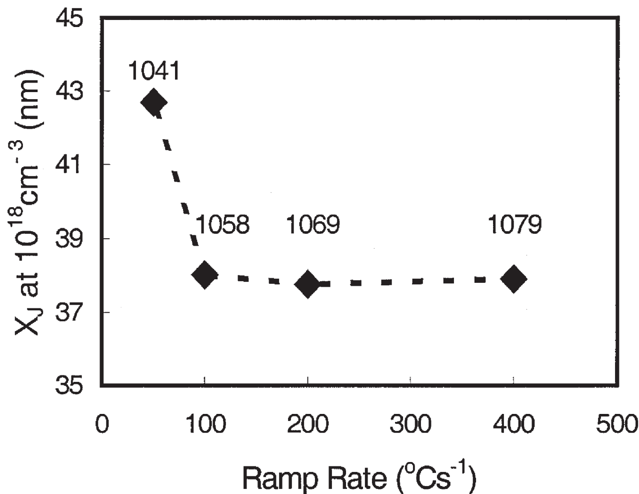

Fig. 4. The junction depths from SIMS analysis for a 0.5-keV, 10^{15} cm^{-2} B^+ implant spike annealed by arc lamp at ramp rates of 50°C, 100°C, 200°C, and 400°C/sec. Peak temperatures (°C) are shown next to symbols and were adjusted to yield constant sheet resistance, Rs = 550 Ω/Sq.

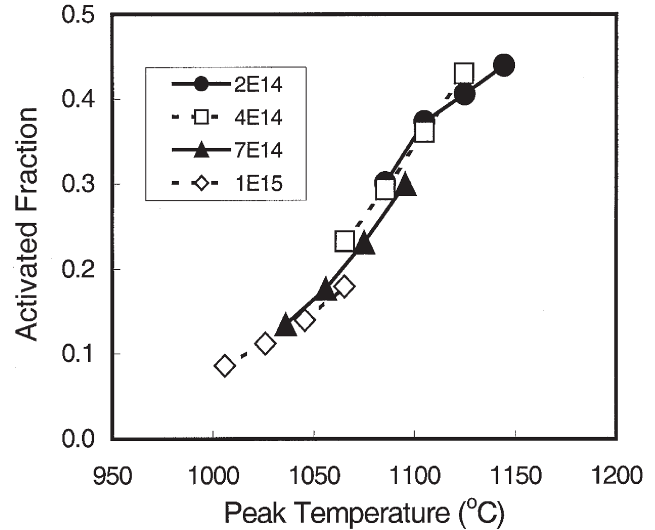

Fig. 5. The activated fraction, determined as ratio of Hall carrier density and implant dose, versus arc-lamp spike-anneal peak temperature for 0.5-keV B^+ implants at four doses indicated (cm^{-2} units).

implant/anneal combination, and data for statistical outliers were discarded. These results are shown in Fig. 6. Junction leakage tends to be lowest at the highest anneal temperatures. Higher leakage at some of the lower spike-anneal temperatures is possibly related to defects in the junctions.

PHOSPHORUS AND ARSENIC IMPLANTS

The experimental picture for low-energy P^+ implants is not as well studied as the case for B^+. For example, it is not known if there is an analog to BED, even though excess Si interstitials contribute to enhanced diffusion of P.[2,3,11,12] Diffusion of n-type dopants was studied for 1.5-keV P^+ and 5-keV As^+ implants. Figure 7 shows that the behavior of 1.5-keV P^+ implants with spike annealing is quite different from that of 0.5-keV B^+ implants. The activated fractions for both B^+ and P^+ implants rapidly increase with peak temperature. However, the activated fractions for various P^+ doses do not overlap

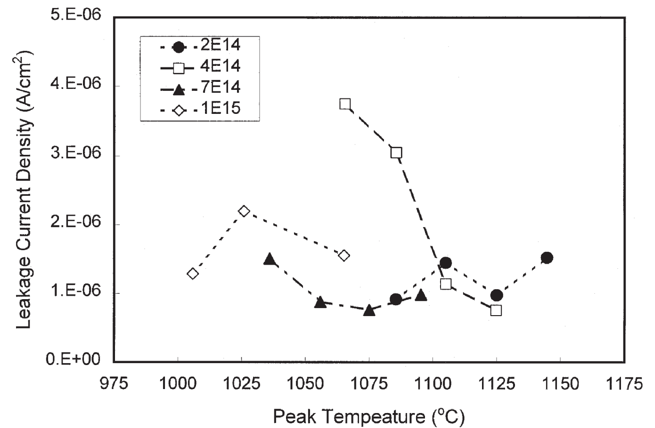

Fig. 6. The reverse-bias, diode-leakage current density (at −1-V bias) versus arc-lamp spike-anneal temperature for 0.5-keV B^+ implants at four doses indicated (cm^{-2} units).

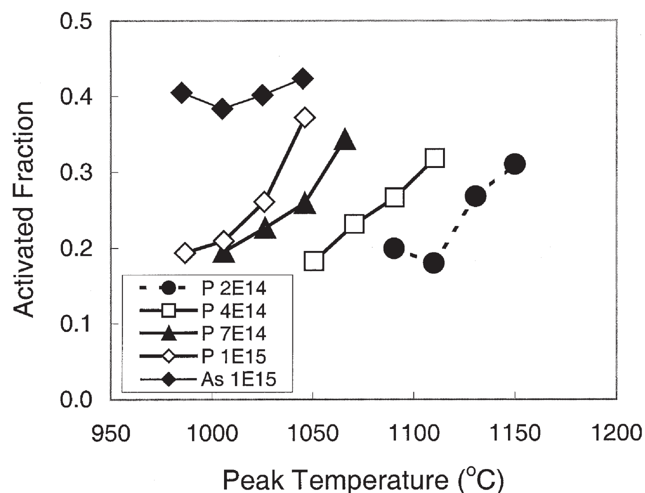

Fig. 7. The activated fraction (Hall carrier density divided by implant dose) versus arc-lamp spike-anneal temperature for 1.5-keV P^+ implants at four doses indicated (cm^{-2} units) and for a 5-keV, 1×10^{15} cm^{-2} As^+ implant.

as they do for the B^+ implants (compare Fig. 5) and, thus, exhibit a strong dependence on implant dose. The active carrier concentration, therefore, varies more rapidly than linearly with implanted P^+ dose. Figure 7 also shows the temperature dependence for a 5-keV As^+ implant at 10^{15} cm^{-2} dose. The As^+ implant yields a higher activated fraction than P^+ implants annealed at the same temperature. Moreover, the activated fraction for As^+ varies by only $\pm 5\%$ with spike-anneal peak temperature, whereas for P^+, at the same dose and same temperature range, it increases monotonically by almost 100%.

The diffusion associated with electrical activation of approximately 25% of the P dopant was examined by SIMS measurements, and the data are shown in Fig. 8. The diffusion depths are fairly insensitive to dose: the depth corresponding to 10^{18} cm^{-3} P concentration varies from 90–100 nm. Using the process simulator PROPHET[4] (Agere Systems, Allentown, PA) to emulate coupled diffusion between P and Si interstitials, we estimate that there is an excess Si-interstitial population of 6–10% of the implanted-P dose. For spike anneals at 1,025°C of 10^{15} cm^{-2} implanted doses, the depth is 32 nm for the As^+ implant and 96 nm for the P^+ implant. The respective sheet resistances are 351 Ω/Sq and 339 Ω/Sq. Thus, higher activation and significantly less diffusion are obtained with the As^+ species.

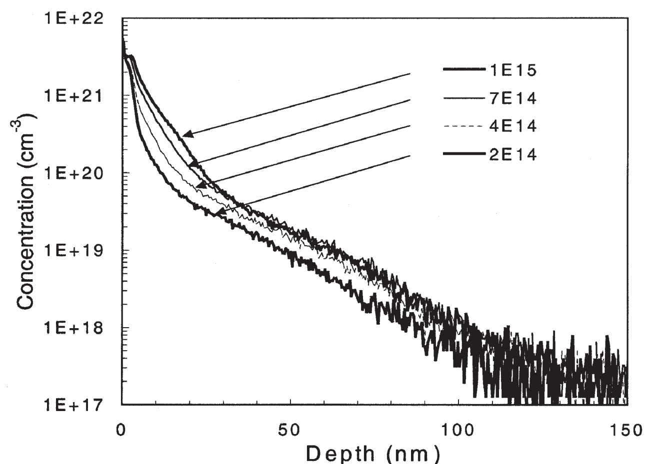

Fig. 8. The SIMS measurements of ^{31}P (includes ^{30}Si) profiles for 1.5-keV P^+ implants after spike annealing. The doses are 0.2, 0.4, 0.7, and 1×10^{15} cm^{-2}. The respective anneal temperatures are 1,131°C, 1,091°C, 1,046°C, and 1,026°C and correspond to electrical activation of approximately 25% of the P.

The variation of sheet resistance and temperature with implant dose for anneals that activate ~25% of the P are shown in Fig. 9. The corresponding spike-anneal temperature decreases monotonically with dose from 1,130–1,025°C, while the sheet resistance also decreases. Results of the reverse-bias diode-leakage current densities, plotted in Fig. 10, show maxima that occur systematically near 25% activation (Fig. 7). The leakage maxima indicate the presence of lattice defects, which may need to be taken into account in modeling TED of P.[11] Figure 10 also shows that junction-leakage results for the As^+ im-

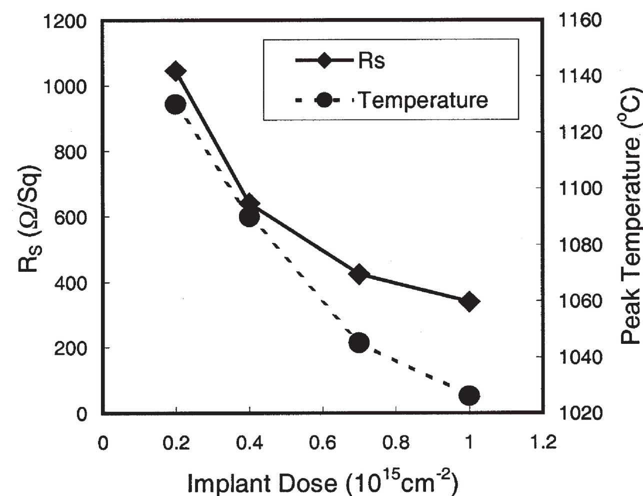

Fig. 9. The variation of sheet resistance and anneal temperature with P dose for arc-lamp spike anneals that activate ~25% of the dose for 1.5-keV P^+ implants.

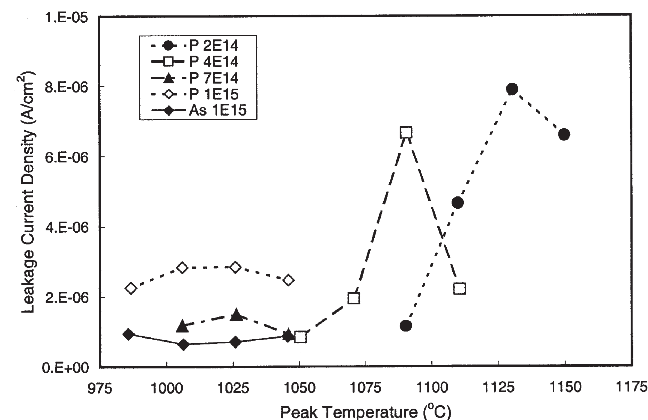

Fig. 10. The reverse-bias diode-leakage current density (at +1-V bias) versus arc-lamp spike-anneal temperature for 1.5-keV P^+ implants at four doses indicated (cm^{-2} units) and 5-keV As^+ implant at 10^{15} cm^{-2} dose.

plant are lower than for P^+ implants at a comparable dose. The near absence of enhanced diffusion and the higher dopant activation makes As the species of choice for shallow n-type extensions.

CONCLUSIONS

Transient-enhanced diffusion, dopant activation, and junction-leakage effects were examined for low-energy implants in Si: 0.5-keV B^+, 1.5-keV P^+, and 5-keV As^+. For spike annealing of B^+ and P^+ implants in the dose range of $0.2–1 \times 10^{15}$ cm^{-2}, the activated fractions increase strongly with peak temperature. Comparing results under similar annealing conditions, the activated fraction of B^+ tends to be constant to within $\pm 10\%$ as a function of implant dose, whereas for P^+ the activated fraction increases strongly with implant dose. The TED of P, which shows weak dose dependence on the diffusion depth, can be modeled with an initial Si-interstitial population estimated to be 6–10% of the implanted dose. The junction leakage observed for P^+ implants is on average two times larger than for B^+ implants and four times larger than for the As^+ implant. Generally, the observed leakage levels are acceptable for ultra-shallow junctions. For spike anneals of 10^{15} cm^{-2} dose implants in the range 985–1,050°C, the As^+ implant shows the highest activation, weakest temperature sensitivity, lowest reverse-bias junction leakage, and minimal transient diffusion.

REFERENCES

1. S. Saito, S. Shishiguchi, A. Mineji, and T. Matsuda, *Mater. Res. Soc. Symp. Proc.* 532, 3 (1998).
2. N.E.B. Cowern, D.J. Godfrey, and D.E. Sykes, *Appl. Phys. Lett.* 49, 1711 (1986).
3. M.D. Giles, *Appl. Phys. Lett.* 62, 1940 (1993).
4. C.S. Rafferty, G.H. Gilmer, M. Jaraiz, D.J. Eaglesham, and H.-J. Gossmann, *Appl. Phys. Lett.* 68, 2395 (1996).
5. A. Ural, P.B. Griffin, and J.D. Plummer, *J. Appl. Phys.* 85, 6440 (1999).
6. A. Agarwal, H.-J. Gossmann, D.J. Eaglesham, S.B. Herner, A.T. Fiory, and T.E. Haynes, *Appl. Phys. Lett.* 74, 2331 and 2345 (1999).
7. K. Suzuki, A. Satoh, T. Aoyama, I. Namura, F. Inoue, Y. Kataoka, Y. Tada, and T. Sugii, *J. Electrochem. Soc.* 142, 2786 (1995).
8. A.T. Fiory, K.K. Bourdelle, and P.K. Roy, *Appl. Phys. Lett.* 78, 1071 (2001).
9. A.T. Fiory and K.K. Bourdelle, *Appl. Phys. Lett.* 74, 2658 (1999).
10. A.T. Fiory, K.K. Bourdelle, M.E. LeFrancois, D.M. Camm, and A. Agarwal, *Advances in Rapid Thermal Processing,* ed. F. Roozeboom, J.C. Gelpey, M.C. Ozturk, and J. Nakos (Pennington, NJ: Electrochemical Society, 1999), vol. PV 99–10, pp. 133–140.
11. M. Uematsu, *Jpn. J. Appl. Phys.* 38, 6188 (1999).
12. X.-Y. Liu, W. Windl, and M.P. Masquelier, *Materials Research Society Symp. Proc.* (Warrendale, PA: Materials Research Society, 2002), vol. 717, pp. C.4.7.1–C.4.7.6.